Energy Science

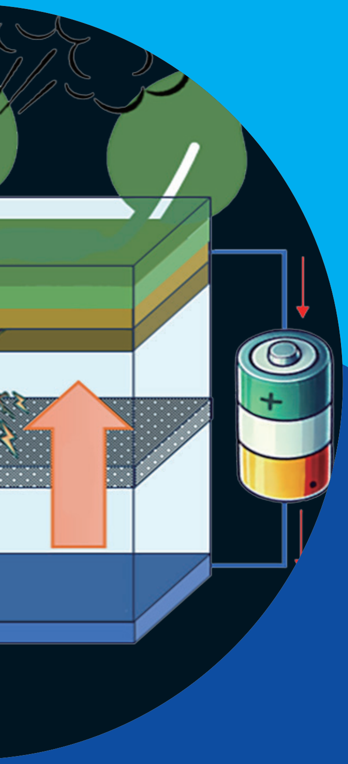

Synchrotron-based techniques remain indispensable in advancing energy storage and catalysis research despite significant progress in computational modeling and emerging *in situ* characterization methods. These techniques provide atomic-level insights into the structural and electronic properties of materials, thus enabling the development of high-performance batteries, electrocatalysts, and photocatalysts. At the NSRRC, several beamlines are dedicated to energy-related research, supporting breakthroughs in sodium ion batteries, zinc–air batteries, photocatalysis, methanol decomposition, and CO_2 electroreduction. Researchers have leveraged X-ray absorption spectroscopy, X-ray photoelectron spectroscopy, and X-ray diffraction to explore material transformations during operation, shedding light on reaction mechanisms and structural stability. **TPS 32A** and **TPS 44A** have been instrumental in characterizing the electronic structure of target materials and have provided crucial insights into defect-engineered nanosheets, which have optimized piezoelectric polarization in the field of sustainable electrocatalysis. **TLS 17C1** has enabled atomic-scale studies of Fe–Co and Ni–Fe bifunctional catalysts, thereby improving oxygen evolution and reduction reactions for zinc–air batteries. **TLS 09A2** and **TLS 24A1** have facilitated research on revealing the role of undercoordinated platinum sites in methanol decomposition. NSRRC's state-of-the-art beamlines continue to support diverse scientific endeavors, enabling fundamental discoveries that drive advancements in sustainable-energy solutions.

In 2024, researchers utilizing NSRRC facilities achieved significant breakthroughs in energy storage and catalytic applications. This report highlights five outstanding contributions that advance battery technology and catalysis for sustainable-energy solutions. The first direction, led by Han-Yi Chen and Ji Liang, addressed a major limitation in current sodium ion transport technology within cathodes. Their work underscored the potential of layered structures, particularly layered metal oxide cathodes with complex elemental compositions, to enhance conductivity, stability, and overall performance. The second direction, headed by Shih-Yuan Lu and Yuan-Yao Li, introduced synergistic binary single-atom catalysts as air cathodes for high-performance and ultrastable zinc–air batteries. This dual-functional system significantly improved the efficiency and rechargeability of zinc–air and aluminum–air batteries, thus paving the way for flexible and sustainable energy storage solutions. For the third direction, Jih-Jen Wu developed dual-vacancy-engineered $ZnIn_2S_4$ nanosheets for hydrogen evolution. This study revealed a novel mechanism where low-frequency-vibration-induced piezoelectric polarization coupled with a static dipole field enhances photocatalytic hydrogen production. For the fourth direction, Meng-Fan Luo investigated undercoordinated Pt sites on the surface of layered $PtTe_2$, elucidating their role in methanol decomposition. This work provided crucial insights into catalytic activity modulation, which can lead to more efficient methanol-to-energy conversion technologies. Finally, Bing Joe Hwang's study introduced a dual single-atom Ni/Cu catalyst that demonstrated highly selective CO_2-to-ethanol conversion. This research represents a major step forward in carbon capture and utilization, offering a promising route for sustainable fuel production. These studies underscore the vital role of NSRRC facilities in advancing battery technology and catalysis, which thereby contributes to the global pursuit of sustainable and efficient energy solutions. (by Hao Ming Chen)

Innovating Sodium-Ion Battery Cathodes: Enhancing Stability and Performance

Layered metal oxide cathode material engineering for sodium ion batteries holds significant potential for alkali-doped P2 and O3 high-capacity layered oxides.

With the rise in the global reliance on renewable energy sources, the demand for cost-effective, scalable energy-storage solutions has increased. Traditional lithium ion batteries (LIBs), while effective, face resource limitations due to lithium's limited supply and mining complexities. By contrast, sodium (Na) is the sixth most abundant element on Earth, making sodium ion batteries (SIBs) a cheaper, highly safe, and more sustainable alternative for large-scale energy-storage applications (**Fig. 1**).[1] The performance of SIBs is considerably influenced by the components of the cathode, anode, and electrolyte. However, achieving the energy densities and performance levels of SIBs comparable to LIBs has been challenging, necessitating extensive research into material compositions, structural arrangements, and electrochemical behaviors of Na ion systems. One of the focal points of recent research on SIBs has been the layered P2 and O3 structures in metal oxide cathode materials, which describe how sodium and transition-metal oxides are arranged within the cathode. In this context, "P" indicates sodium ions positioned at prismatic sites, while "O" indicates those located at octahedral sites based on the stacking sequences of oxide layers. The numbers 2 and 3 represent the number of Na ion layers per unit cell. Recently, most researchers have been exploring the ways to modify the layered structures and develop hybrid models to capitalize on each structure's strengths, aiming to suppress the adverse phase transition of layered oxide cathodes. For instance, inserting or doping alkali or transition-metal cations in the layered structure, designing a multi-element intention known as a high-entropy system, and switching between O3 and P2 phases during operation can, in theory, provide the high specific capacities for efficient energy storage and exhibit excellent cycling stability for reliable performance over multiple charge–discharge cycles. Variations of designs remain an area of active investigation, with potential implications for improving SIB performance. Employing a combination of advanced synchrotron X-ray techniques, including X-ray photoelectron spectroscopy (XPS), X-ray diffraction (XRD), and X-ray absorption spectroscopy (XAS), plays a key role in examining the structural and electrochemical properties of the layered cathode materials. These techniques allow for in-depth analysis of the materials at an atomic and molecular level, providing insights into their structural stability, chemical composition, and electronic behavior.

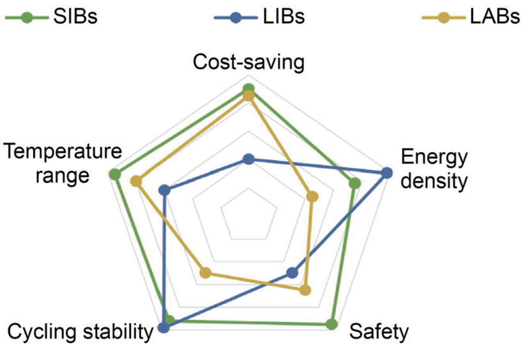

Fig. 1: Comparison of three established rechargeable battery technologies (SIBs, LIBs, and lead–acid batteries (LABs)) in the current market. [Reproduced from Ref. 1]

Most studies have tackled these challenges through innovative cathode material engineering for achieving high energy density and ensuring long-term cycling stability for SIBs. Han-Yi Chen (National Tsing Hua University) focused on a potassium (K)-doped P2-type layered $Na_{0.67}Mg_{1/3-x}Cu_xMn_{2/3}O_2$ oxide cathode, which utilizes alkali-doped configuration to facilitate the movement of Na ions through larger diffusion pathways. This configuration enhances ionic conductivity and improves electrochemical performance.[2] K ions were selected for doping because of their larger ionic radius compared to Na, which thereby serves as a "pillar" that stabilizes the layered structure during Na ion intercalation and deintercalation. In particular, a doping level of $K_{0.05}$ showed the most promising results, achieving the highest specific capacity of 203 mAh/g, which represents a significant improvement compared to the undoped material's capacity of 185 mAh/g. This highlights the effectiveness of K doping in expanding ion diffusion pathways and enhancing material stability. *In situ* XRD analysis conducted at **TLS 01C2** provided insights into structural shifts within the cathode materials, revealing that moderate potassium doping (up to $K_{0.05}$) supports the P2 structure without causing unwanted phase transitions (**Fig. 2**, see next page). XAS analysis of transition-metal K-edges performed at **TPS 44A** and **TLS 17C1** further supported these findings, revealing that potassium doping did not alter the oxidation states of the transition metals. The structural integrity and charge balance were maintained within the material. This result is critical as it demonstrates that potassium serves as a stabilizer without disrupting the essential redox processes in the cathode material.

Another similar research conducted this year by Ji Liang (Tianjin University, China) explored a Li/Ti co-substitution strategy to address structural challenges in O3-type layered oxide cathodes for SIBs.[3] By modifying the local electronic configuration of oxygen in $NaNi_{0.5}Mn_{0.5}O_2$ (NM) with an O3 structure, this approach effectively mitigates phase transitions and enhances structural stability, especially at high voltages, a common problem for layered oxides under high sodium extraction. This is a key development in stabilizing O3-phase materials through the specific elemental substitution. It demonstrates that Li/Ti co-substitution strengthens electrostatic bonding in the transition-metal layer and prevents adverse phase transitions, such as those from O3 to OP2, in a voltage range of 2.0–4.3 V. The Li/Ti-modified $NaLi_{1/9}Ni_{1/3}Mn_{4/9}Ti_{1/9}O2$ (LNMT) cathode achieved impressive electrochemical performance with a capacity of 161.2 mAh g^{-1} at 1C and 80% retention after 100 cycles, underscoring the effectiveness of local electronic regulation in addressing phase instability (**Fig. 3**).

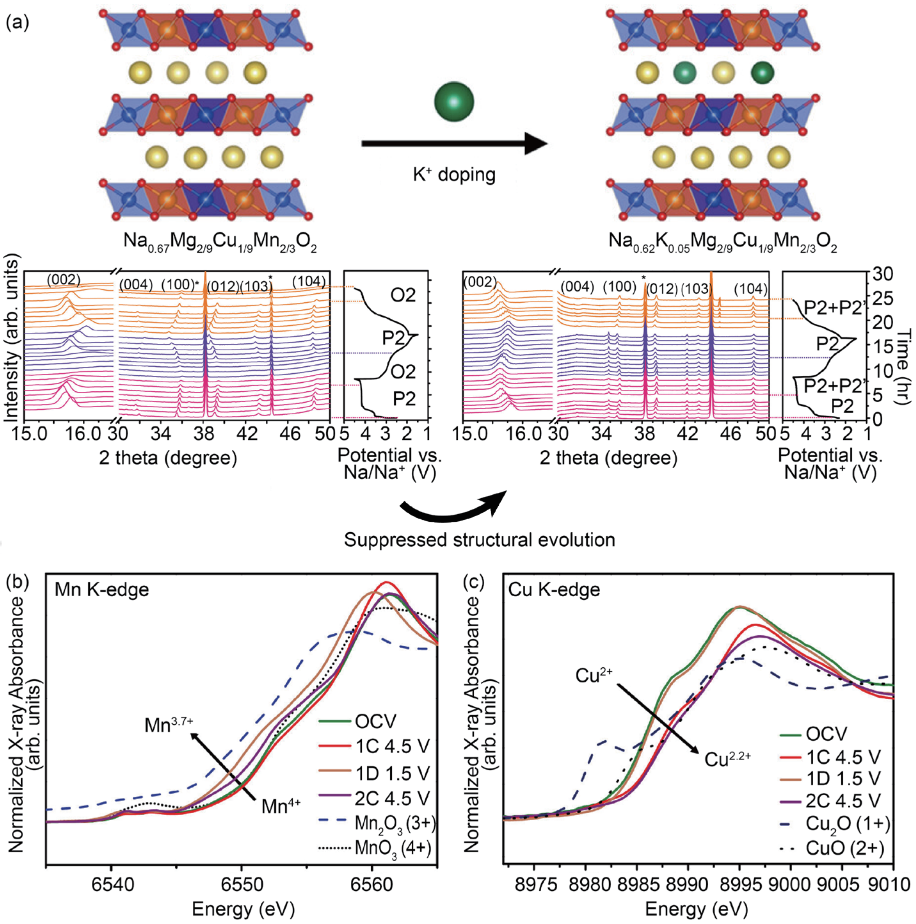

Fig. 2: Schematic K-doped P2 crystal structures and *in situ* XRD patterns of (a) $K_{0.00}$ and $K_{0.05}$. *In situ* XAS spectra of (b) Mn K-edge and (c) Cu K-edge of $K_{0.05}$ during cycling. [Reproduced from Ref. 2]

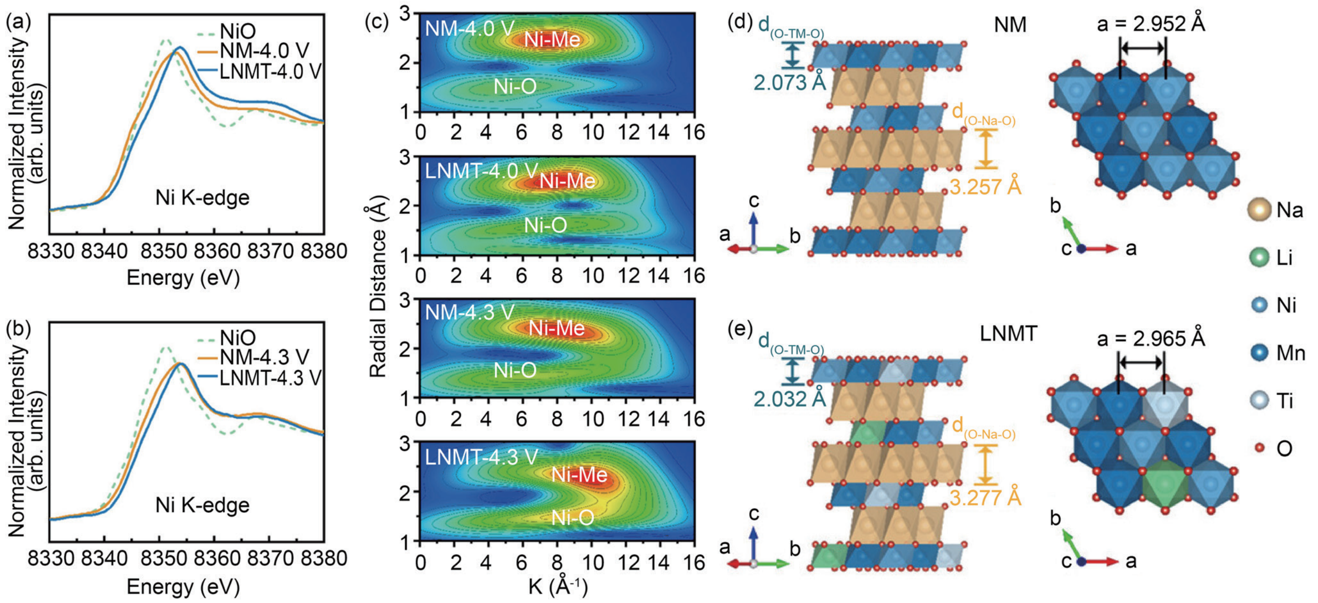

Fig. 3: (a,b) *Ex situ* XANES spectra at Ni K-edge of NM, LNMT, and NiO obtained at different charging conditions. (c) Wavelet transformation diagrams of the NM and LNMT under different voltage states. Schematic crystal structures and detailed lattice parameters of (d) NM and (e) LNMT. [Reproduced from Ref. 3]

XAS analysis conducted at **TPS 32A** revealed that LNMT promotes a stable electronic environment, mitigates drastic structural changes, and supports a more robust charge compensation mechanism. These findings highlight the importance of fine-tuning local electronic and atomic structures in designing high-capacity, high-voltage SIB cathodes. Together, these studies offer key insights into the effects of local structure on the electrochemical behavior of layered oxide cathodes, thereby paving the way for new developments in energy-storage solutions that offer enhanced capacity and cycle life.

In conclusion, while developing high-capacity and long-cycle-life SIBs remains challenging, addressing one of the major limitations of the current sodium ion transport technology in the cathodes highlights the potential of layered structures. Investigating the impact of these layered metal oxide cathodes with complex element compounds could potentially enhance the conductivity, stability, and overall performance. Applying *in situ* synchrotron X-ray techniques is essential for monitoring SIB behavior during operation. These methods provide valuable insights into changes that occur during charge–discharge cycles, enabling researchers to customize materials for improved performance. By combining the strengths of these configurations and leveraging advanced synchrotron X-ray techniques, the research lays the groundwork for more efficient, durable, and economically viable SIBs. (Reported by Chi-Liang Chen)

This report features the work of Han-Yi Chen and her collaborators published in ACS Sustain. Chem. Eng. ***12****, 12795 (2024), and the work of Ji Liang and his collaborators published in ACS Nano* ***18****, 18622 (2024).*

TPS 32A Tender X-ray Absorption Spectroscopy
TPS 44A Quick-scanning X-ray Absorption Spectroscopy
TLS 17C1 EXAFS
TLS 01C2 X-ray Powder Diffraction

- XPS, XRD, XAS
- Energy Science, Chemistry, Materials Science, Condensed Matter

References

1. L. Zhao, T. Zhang, W. Li, T. Li, L. Zhang, X. Zhang, Z. Wang, Engineering **24**, 172 (2023).
2. C.-H. Yeh, J.-W. Kang, Y.-L. Chen, H.-J. Chen, H.-H. Chang, W.-H. Lu, S.-Y. Chen, H.-L. Chen, C.-W. Hu, L.-Y. Chueh, Y.-T. F. Pan, H.-Y. Chen, ACS Sustain. Chem. Eng. **12**, 12795 (2024).
3. Q. Wang, G. Yu, B. Luo, W. Ji, Z. Liu, M. Li, Y. Nong, Y. Tian, X. Wang, J. Zhang, C.-L. Chen, C.-K. Chang, Z. Sang, Z. Zhao, R. Zhao, J. Liang, ACS Nano **18**, 18622 (2024).

Breathing Zinc–Air Batteries: Clean, Powerful, and Sustainable Energy Solutions

The development of advanced bifunctional catalysts is essential for attaining high-performance cathodes in rechargeable zinc-air batteries.

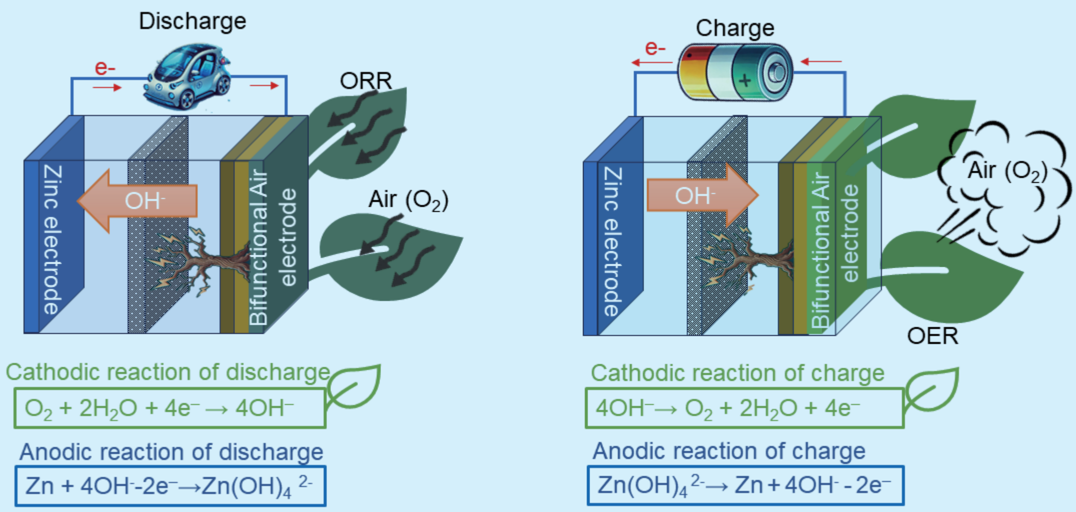

Fig. 1: A schematic configuration of zinc–air batteries and oxygen bifunctional electrocatalysts.

Zinc–air batteries (ZABs), a type of metal–air battery, generate electricity by combining zinc (Zn) with oxygen (O_2) from the air. At their core, these batteries consist of a Zn anode, a porous air cathode, and an electrolyte, which is often a strong alkaline solution. During discharge, zinc oxidizes at the anode, releasing electrons that travel through an external circuit to the cathode. Simultaneously, oxygen molecules from the air reduce at the cathode, combining with water and electrons to form hydroxide ions. These ions react with Zn ions in the electrolyte to form zincates (**Fig. 1**). This process releases energy that powers devices. ZABs are appealing for energy-intensive applications such as electric vehicles, grid energy storage, and portable devices. With a theoretical energy density potentially exceeding 1,000 Wh/kg, ZABs surpass lithium ion batteries. However, challenges in rechargeability and stability have historically hindered their commercial viability. Key limitations of ZABs include the rechargeability of the zinc anode and the sluggish oxygen reduction reaction (ORR) and oxygen evolution reaction (OER) kinetics at the cathode. Repeated charge–discharge cycles can lead to zinc dendrite formation, causing short circuits. In addition, reactions between zinc and the alkaline electrolyte can produce by-products that degrade performance. To address these issues, recent research has focused on improving the electrolyte, cathode catalysts, and zinc anode structure. Promising developments include the use of solid-state electrolytes to minimize side reactions and innovative anode designs to prevent dendrite formation. Particularly, enhancing cathode catalysts to improve ORR and OER efficiency is a critical area of research for bifunctional electrocatalysts. Synchrotron X-ray absorption spectroscopy (XAS), which includes X-ray absorption near edge structure (XANES) and extended X-ray absorption fine structure (EXAFS) analyses, provides the valuable insights. XAS examines the oxidation state, electronic properties, atomic coordination, and bond lengths of

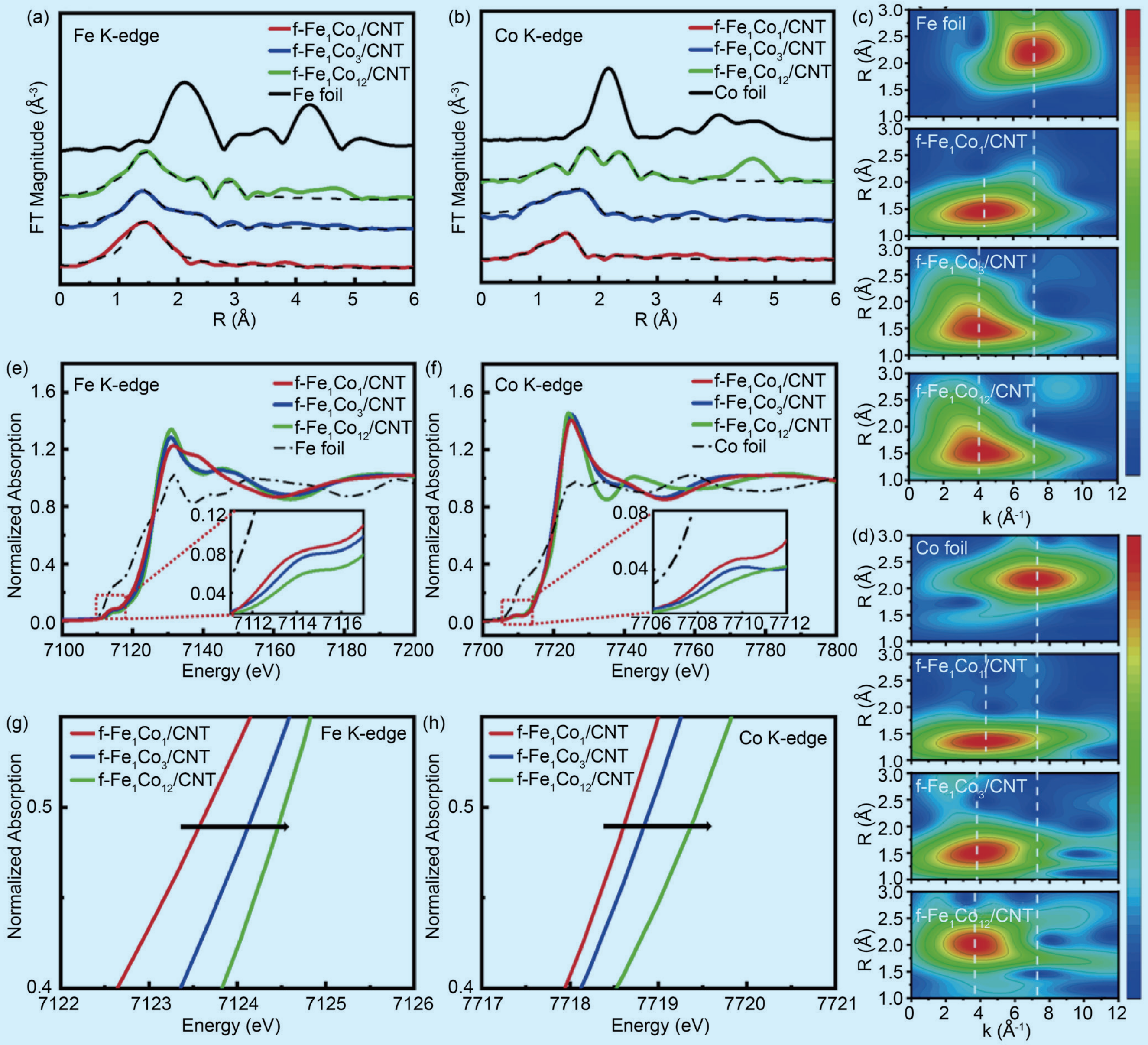

Fig. 2: EXAFS k^2-weighted R-space results for (a) Fe K-edge and (b) Co K-edge, including fitted curves (black dashed lines). (c,d) k^2-weighted WT images for the Fe and Co K-edges. (e,f) XAS spectra, with insets highlighting pre-edge peaks and (g,h) absorption edges. [Reproduced from Ref. 1]

catalyst atoms. This detailed understanding is essential for the rational design of more efficient catalysts by elucidating the relationships between the structure and properties, as it reveals the atomic structure and electronic properties. This analysis also sheds light on how these factors influence catalytic performance through a comprehensive analysis of the underlying mechanisms. Some ZABs have achieved impressive cycling stability and reaction efficiency this year, outperforming traditional and commercial Pt/C + IrO_2 catalysts. Therefore, if these innovations continue, ZABs could emerge as mainstream alternatives to lithium ion batteries in the near future.

Shih-Yuan Lu (National Tsing Hua University) investigated a binary Fe and Co single-atom catalyst (SAC) named f-Fe_1Co_1/CNT. This catalyst, which is synthesized *via* a formamide-assisted solvothermal approach and analyzed using XAS at **TLS 17C1**, anchors Fe and Co single atoms on nitrogen-doped carbon layers supported by carbon nanotubes (CNTs). This design achieves high atom loading and prevents aggregation, significantly enhancing ORR and OER efficiency in alkaline media. The f-Fe_1Co_1/CNT catalyst demonstrates superior ORR and OER activities and achieves the remarkable discharge peak power density and stability when paired with a carbon-paper-composited nickel foam (NF/CP) air cathode. XAS analysis, including EXAFS and wavelet-transform (WT) analysis, confirmed the changes in coordination environments and revealed synergistic activity from Fe and Co atoms, with Fe-N_4 sites identified as the primary active centers. These findings highlight the potential of SACs to achieve high catalytic activity, selectivity, and stability.

Furthermore, this year, noteworthy research conducted by Yuan-Yao Li (National Chung Cheng University) introduced a sophisticated bifunctional catalyst that integrates nickel–iron-layered double hydroxide (NiFe LDH), iron–cobalt dual single atoms (FeSACoSA), and iron–cobalt nanoalloy (FeCoAlloy) within a framework of nitrogen-doped carbon (NC) and CNTs. This combination maximizes the ORR and OER activities by leveraging the synergistic properties of its components, notably, the high density of ORR active sites provided by the FeCo alloy and FeSACoSA and the enhanced durability and OER efficiency contributed by NiFe LDH. The low ORR–OER potential gap of the catalyst and its implementation in a conductive, porous cathode structure deliver the outstanding performance in liquid-state and flexible ZABs. Such ZABs achieve impressive power densities, specific capacities, and cycling stability surpassing commercial benchmarks. **Figure 3** presents the results of XAS analysis conducted at **TLS 17C1**. The Co and Fe K-edge results revealed the presence of metal–metal bonds, confirming both metal-N coordination and the existence of an FeCo alloy within the material. Furthermore, the Ni K-edge spectra exhibited Ni–O and Ni–Ni bonds from NiFe LDH, confirming the successful coating of NiFe LDH on the material. These findings highlight the importance of both single-atom dispersion and synergistic interactions between the different active sites in achieving high catalytic efficiency in these binary SACs.

The development of ZABs highlights the potential of advanced catalyst–cathode configurations. Utilizing synchrotron XAS to analyze catalytic mechanisms can drive further advancements. With continuous improvements in bifunctional catalysts,

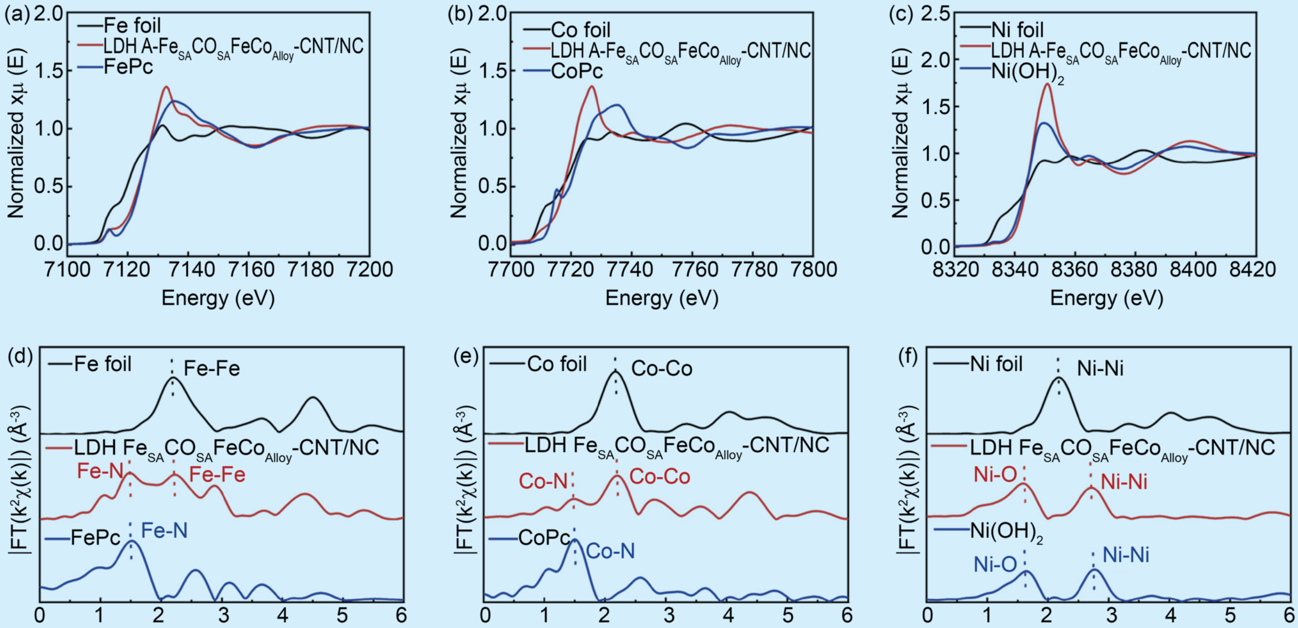

Fig. 3: XAS spectra of NiFe LDH A-FeSACoSA-FeCo Alloy CNT/NC. XANES spectra for (a) Fe K-edge, (b) Co K-edge, and (c) Ni K-edge. Fourier transform EXAFS spectra for (d) Fe K-edge, (e) Co K-edge, and (f) Ni K-edge. [Reproduced from Ref. 2]

ZABs may soon emerge as a viable solution for large-scale energy storage and transportation. Combining high energy density, eco-friendly materials, and reduced costs, ZABs hold promise as a cornerstone of sustainable energy solutions. (Reported by Chi-Liang Chen)

This report features the work of Shih-Yuan Lu and his collaborators published in Energy Storage Mater. ***67****, 103286 (2024), and the work of Yuan-Yao Li and his collaborators published in Nano Energy* ***121****, 109236 (2024).*

TLS 17C1 EXAFS

- XAS, WT
- Materials Science, Chemistry, Condensed-matter Physics

References

1. Y.-C. Ting, C.-C. Cheng, S.-H. Lin, T.-Y. Lin, P.-W. Chen, F.-Y. Yen, S.-I Chang, C.-H. Lee, H.-Y. T. Chen, S.-Y. Lu, Energy Storage Mater. **67**, 103286 (2024).
2. W.-X. Hong, W.-H. Wang, Y.-H. Chang, H. Pourzolfaghar, I-H. Tseng, Y.-Y. Li, Nano Energy **121**, 109236 (2024).

Novel $ZnIn_2S_4$ Combines Piezopotential and Dipole Field for Hydrogen Technique

This study offers an in-depth examination of vacancy engineering in ZIS nanosheets, utilizing piezopotential and dipole fields to optimize photocatalytic performance.

Visible-light-driven photocatalysts often suffer from significant charge recombination due to their limited carrier diffusion lengths, which constrain their practical applications. A common strategy for mitigating this challenge is the development of heterostructure photocatalysts with built-in junction fields to promote charge separation. Alternatively, leveraging the dipole field within the internal bulk phase of photocatalysts has demonstrated considerable effectiveness in enhancing charge separation and transport. This dipole field arises naturally in photocatalysts with non-centrosymmetric crystal structures and can be introduced through the structural modifications. Piezoelectric polarization, a macroscopic built-in potential, is generated in piezoelectric crystals with non-centrosymmetric structures in response to applied mechanical stress. Piezo-photocatalysis synergistically integrates the piezoelectric effect with the light-harvesting capabilities of piezoelectric semiconductors, facilitating the separation and movement of photogenerated charge carriers through the macroscopic built-in potential field.

Jih-Jen Wu (National Cheng Kung University) and his coworkers recently investigated the influence of In- and S-vacancy concentrations on the photocatalytic activity of zinc indium sulfide (ZIS) nanosheets for hydrogen evolution reactions (HERs). Using X-ray absorption spectroscopy (XAS) measurements, including X-ray absorption near edge structure (XANES) and extended X-ray absorption fine structure (EXAFS), conducted at **TPS 32A** and **TPS 44A**,[1] they gained deeper insights into the structural transformations of defective ZIS after hydrazine treatment. For clarity, the unmodified ZIS powder, as well as the modified ZIS powders that had been subjected to hydrazine treatment for 1 hour and 5 hours, are designated as ZIS-0, ZIS-1, and ZIS-5, respectively. **Figure 1(a)** presents the XANES spectra of the ZIS samples at the S K-edge, revealing a notable increase in sulfur vacancies and unoccupied states at sulfur sites following hydrazine treatment. **Figures 1(b) and 1(c)** illustrate the XANES and EXAFS spectra at the Zn K-edge for ZIS-0 and ZIS-5. The reduced coordination number and elevated electron density observed at Zn sites in ZIS-5 compared to ZIS-0 are attributed to the higher concentration of sulfur vacancies in ZIS-5. Similarly, **Figs. 1(d) and 1(e)** display the XANES and EXAFS spectra at the In K-edge for ZIS-0 and ZIS-5. Because of the contrasting trends in electron density changes driven by sulfur and indium vacancies, it was determined that sulfur vacancies have a more pronounced effect on the electron density at the indium sites in ZIS-5 than do indium vacancies, resulting in increased electron density at these sites compared to ZIS-0. Additionally, ZIS-5 exhibits a slightly diminished sulfur coordination environment relative to ZIS-0, which is attributed to a higher sulfur vacancy concentration post-treatment. The atomic arrangement of sulfur and indium vacancies within

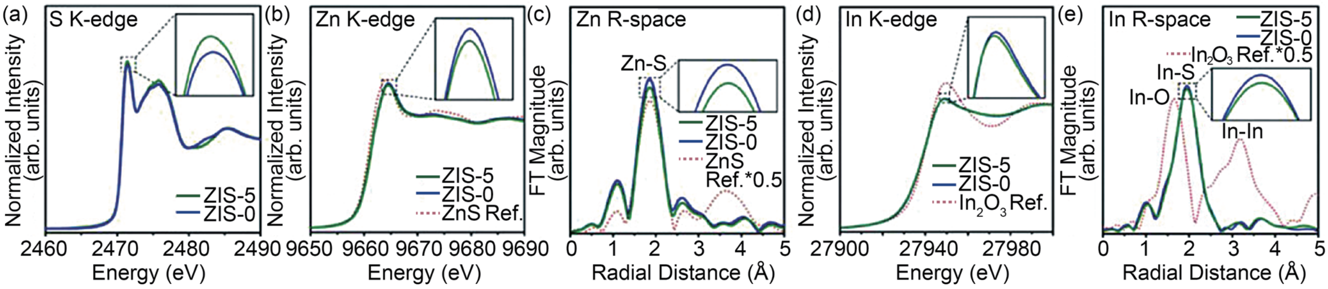

Fig. 1: (a) Normalized S K-edge XANES spectra for ZIS-0 and ZIS-5. (b) Normalized Zn K-edge XANES spectra and (c) Fourier transformed (FT) EXAFS spectra in R-space of ZIS-0, ZIS-5, and ZnS reference. (d) Normalized In K-edge XANES spectra and (e) FT EXAFS spectra in R-space of ZIS-0, ZIS-5, and In_2S_3 reference. [Reproduced from Ref. 1]

the ZIS structure plays a pivotal role in facilitating rapid charge transfer and effective charge separation, ultimately enhancing hydrogen production. This investigation meticulously explores how sulfur and indium vacancies improve charge dynamics and hydrogen evolution rates. By integrating the experimental data with multi-scale simulations, the study demonstrates how these vacancies optimize hydrogen production, offering valuable insights into the mechanisms by which structural vacancies in ZIS influence its electrochemical performance, particularly in hydrogen generation applications.

In summary, defect engineering of ZIS nanosheets with varying levels of indium and sulfur vacancies was successfully realized through hydrazine post-treatment of hydrothermally synthesized ZIS nanosheets. The photocatalytic HER rates show a positive correlation with the combined concentrations of indium and sulfur vacancies in the ZIS nanosheets. This study provides a detailed exploration of vacancy engineering in ZIS nanosheets, leveraging piezoelectric polarization in conjunction with the dipole field to enhance photocatalytic efficiency. (Reported by Yan-Gu Lin)

This report features the work of Jih-Jen Wu and his coworkers published in Adv. Mater. ***36****, 2403228 (2024).*

TPS 32A Tender X-ray Absorption Spectroscopy
TPS 44A Quick-scanning X-ray Absorption Spectroscopy

- XAS
- Materials Science, Chemistry, Condensed-matter Physics, Environmental and Earth Science

Reference

1. W. J. Zhong, M. Y. Hung, Y. T. Kuo, H. K. Tian, C. N. Tsai, C. J. Wu, Y. D. Lin, H. C. Yu, Y. G. Lin, J. J. Wu, Adv. Mater. **36**, 2403228 (2024).

Defect-Engineering for Selective Methanol Decomposition

Undercoordinated Pt sites in $PtTe_2$ are crucial in facilitating methanol decomposition and promoting formaldehyde production.

Two-dimensional transition metal dichalcogenides (TMDs) have garnered significant attentions in catalysis due to their unique electronic properties, high surface area, and tunable surface chemistry. Unlike conventional noble metal catalysts, which exhibit disadvantages such as high costs and susceptibility to poisoning, TMDs are promising alternatives owing to their structural versatility and defect engineering capabilities.[1,2] However, the basal planes of pristine TMDs are often inert, limiting their catalytic utility. Surface defects, particularly chalcogen vacancies, introduce the undercoordinated metal sites that can serve as highly active catalytic centers, significantly altering their chemical reactivity. Among TMDs, platinum telluride ($PtTe_2$) is of particular interest due to its intrinsic metallic nature, which provides superior conductivity compared to semiconducting TMDs such as MoS_2 or WS_2. A research team led by Meng-Fan Luo (National Central University), Jyh-Pin Chou (National Changhua University of Education), and Chun-Liang Lin (National Yang Ming Chiao Tung University) is investigating the catalytic properties of $PtTe_2$ with engineered Te vacancies. Their study focuses on $PtTe_2$, a metallic group-10 TMD, emphasizing the role of undercoordinated Pt (Pt_{uc}) sites at Te vacancies in methanol decomposition, which is a crucial reaction for hydrogen production and direct methanol fuel cells. To explore the catalytic behavior of $PtTe_2$, controlled Ar^+

bombardment was employed to selectively remove surface Te atoms, generating Pt$_{uc}$ sites while maintaining the structural integrity of the underlying Pt lattice. **Figure 1(a)** presents the scanning tunneling microscopy (STM) images before and after ion bombardment, confirming the introduction of single and multi-Te vacancies. **Figure 1(b)** further characterizes the defect structure through synchrotron-based photoelectron spectroscopy (PES), which reveals a shift in the Pt 4f binding energy. This shift indicates a lower oxidation state at Pt$_{uc}$ sites, which enhances their reactivity. To assess the influence of Pt$_{uc}$ concentration on catalytic performance, **Figs. 1(c) and 1(d)** quantify the methanol conversion probability as a function of vacancy density. At low Pt$_{uc}$ concentrations (≤10%), methanol conversion exceeds 90%, with high selectivity toward CH_2O and CH_4. As Pt$_{uc}$ concentration increases (10%–20%), selectivity shifts, favoring C–O bond scission over dehydrogenation, which is further validated by near-ambient-pressure photoelectron spectroscopy (NAP-PES) and near-ambient-pressure mass spectroscopy results.

Methanol adsorption and decomposition were systematically investigated using synchrotron-based *in situ* NAP-PES and near-ambient pressure mass spectrometry (NAP-MS). As shown in **Fig. 2(a)**, the NAP-PES spectra for pristine $PtTe_2$ reveal that methanol does not undergo significant decomposition, confirming its catalytic inertness. In contrast, on defect-rich $PtTe_2$, the spectral intensity of methanol-related species (CH_3OH) decreases with increasing temperature, indicating the progressive methanol conversion. Concomitantly, peaks corresponding to CH_2O (formaldehyde) and CH_x species are observed, which demonstrate that Pt$_{uc}$ sites actively promote methanol dehydrogenation. NAP-MS results further confirm these findings by monitoring the gaseous products formed during the reaction (**Fig. 2(b)**). On Pt$_{uc}$-enriched $PtTe_2$, CH_2O (formaldehyde) and CH_4 (methane) are the dominant products, whereas only trace amounts of CO and CO_2 are detected.

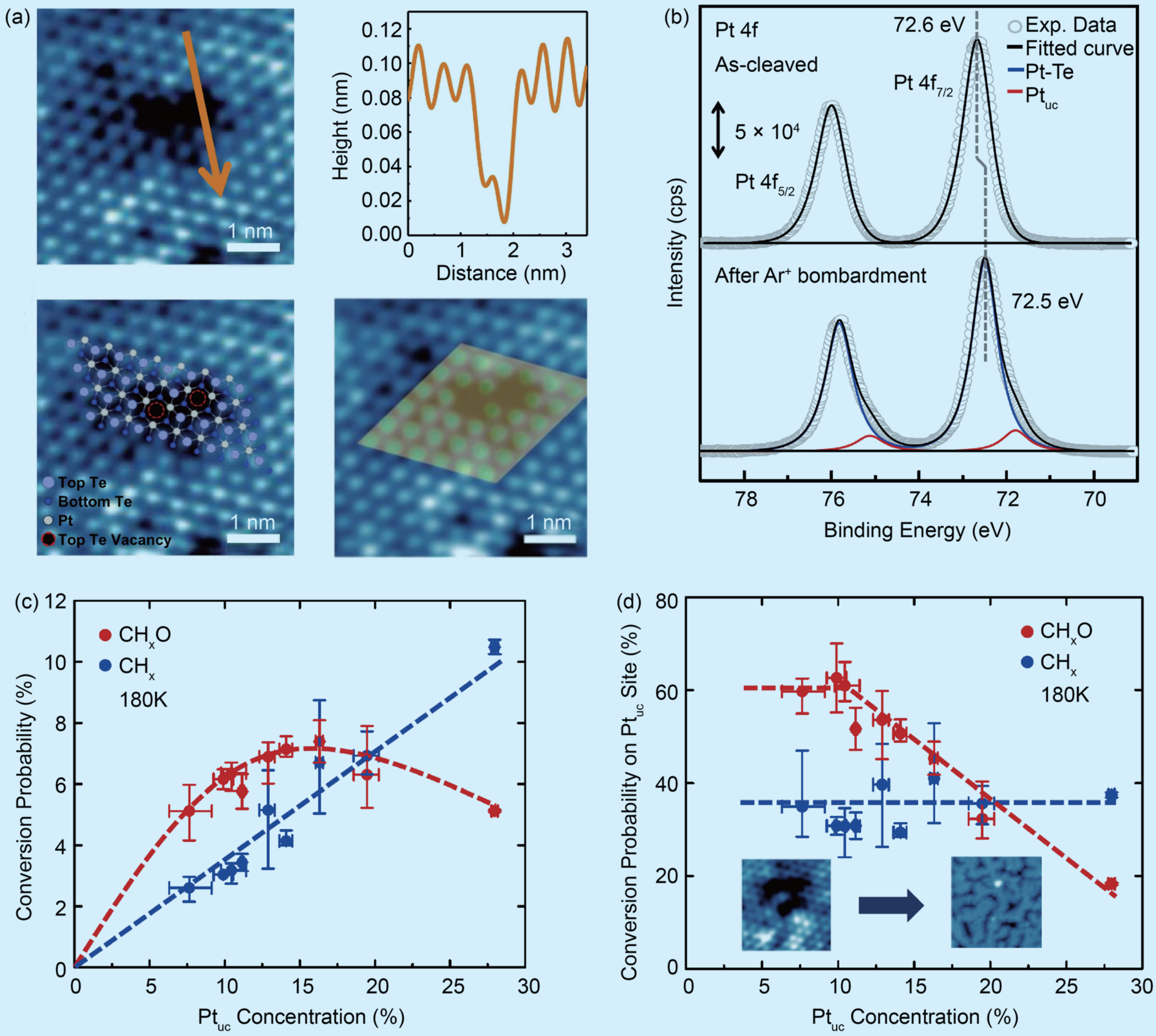

Fig. 1: (a) High-resolution image of two single-Te vacancies, the line profile across a single-Te vacancy, the overlap of the two single-Te vacancies model with the imaged ones and the overlap of the STM image with the DFT-simulated one produced based on the vacancy model. (b) PES spectra of Pt 4 f core level from layered $PtTe_2$ as cleaved and bombarded by Ar$^+$ (0.5 keV, 3 mins). (c,d) Varied reaction probabilities of methanol adsorbed on a $PtTe_2$ surface with Pt$_{uc}$ sites. Probabilities of conversion to CH_xO* (red circles) and CH_x* (blue) of monolayer methanol adsorbed on a $PtTe_2$ surface, and those on Pt$_{uc}$ sites as a function of the concentration of the surface Pt$_{uc}$. [Reproduced from Ref. 3]

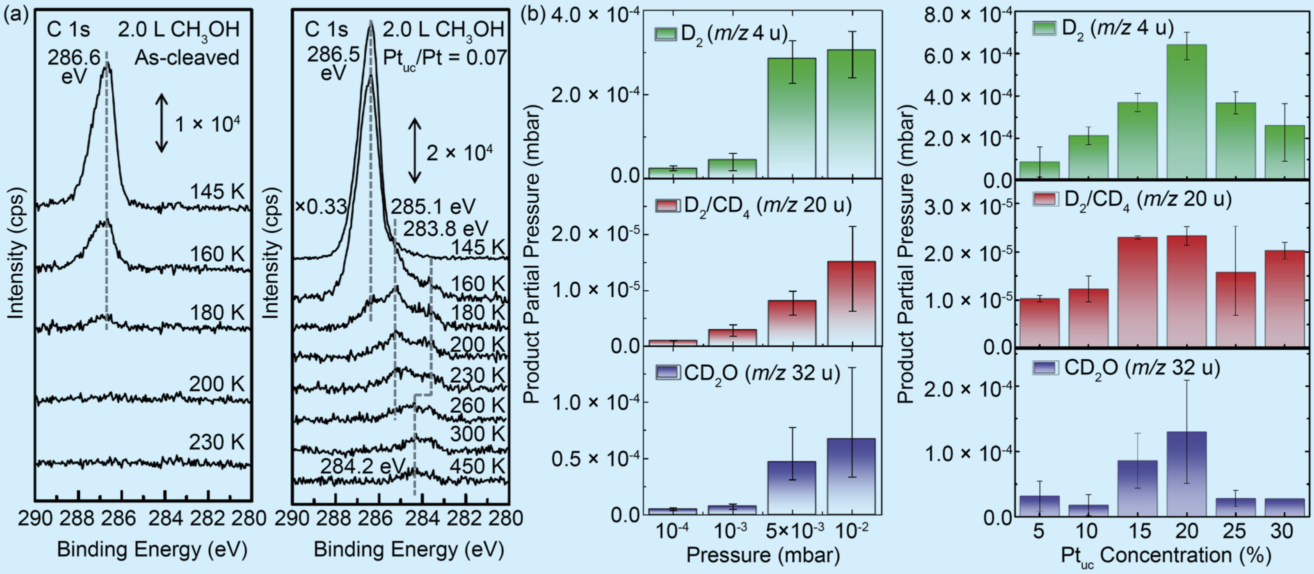

Fig. 2: (a) PES spectra of C 1s core level for methanol adsorbed on as-cleaved and Ar$^+$-bombarded $PtTe_2$ at 145 K and annealed stepwise to selected temperatures. (b) Production of $D_{2(g)}$ (*m/z* 4 u), $D_2O_{(g)}$ /$CD_{4(g)}$ (*m/z* 20 u), and $CD_2O_{(g)}$ (*m/z* 32 u) from $PtTe_2$ at 300 K, as a function of methanol-d_4 pressure (Pt_{uc}/Pt ratio 0.10) and Pt_{uc} concentration (10^{-2} mbar). [Reproduced from Ref. 3]

This highlights the selective nature of Pt_{uc} sites, which favor formaldehyde formation over complete C–O bond scission, reducing unwanted CO poisoning, which is an issue commonly observed for conventional Pt catalysts. Additionally, the reaction selectivity shifts with increasing Pt_{uc} concentration. At moderate defect densities (~10%), methanol decomposition predominantly follows the dehydrogenation pathway, producing CH_2O and CH_4. However, at higher Pt_{uc} densities (>10%), the C–O bond cleavage pathway becomes more competitive, leading to increased CH_4 and H_2 formation while slightly reducing CH_2O selectivity. This trend is consistent with density functional theory (DFT)-calculated reaction barriers, which suggest that Pt_{uc} sites lower the activation energy for selective dehydrogenation but can also facilitate C–O scission at higher defect concentrations.

In summary, this study establishes $PtTe_2$ with undercoordinated Pt sites as a highly efficient catalyst for methanol decomposition, offering superior activity and selectivity compared to conventional Pt catalysts. The unique triangular coordination and oxidation state variations of Pt_{uc} sites play a crucial role in tuning the reaction pathways. By integrating advanced synchrotron-based PES, *in situ* NAP-PES/NAP-MS at **TLS 09A2** and **TLS 24A1**, and theoretical modeling, this work provides fundamental insights into defect engineering in TMDs. It lays the foundation for designing next-generation catalysts for methanol reforming, hydrogen production, and direct methanol fuel cells. (Reported by Hao Ming Chen, National Taiwan University)

This report features the work of Meng-Fan Luo, Jyh-Pin Chou and Chun-Liang Lin published in Nat. Commun. ***15****, 653 (2024).*

TLS 09A2 Spectroscopy
TLS 24A1 XPS, UPS, XAS, APXPS

- *In situ* NAP-XPS
- Materials Science, Thin-film Chemistry

References

1. G. D'Olimpio, C. Guo, C.-N. Kuo, R. Edla, C. S. Lue, L. Ottaviano, P. Torelli, L. Wang, D. W. Boukhvalov, A. Politano, Adv. Funct. Mater. **30**, 1906556 (2020).
2. Y. Chen, S. Huang, X. Ji, K. Adepalli, K. Yin, X. Ling, X. Wang, J. Xue, M. Dresselhaus, J. Kong, B. Yildiz, ACS Nano, **12**, 2569 (2018).
3. J.-W. Hsueh, L.-H. Kuo, P.-H. Chen, W.-H. Chen, C.-Y. Chuang, C.-N. Kuo, C.-S. Lue, Y.-L. Lai, B.-H. Liu, C.-H. Wang, Y.-J. Hsu, C.-L. Lin, J.-P. Chou, M.-F. Luo, Nat. Commun. **15**, 653 (2024).

Dual-Atom Catalyst for Selective CO_2 Reduction

A dual-atom NiCu catalyst achieves record-high selectivity for CO_2-to-ethanol conversion.

The electrochemical reduction of carbon dioxide (CO_2) into valuable multi-carbon fuels is a promising strategy for mitigating CO_2 emissions while producing sustainable chemical feedstocks.[1] However, achieving high selectivity and efficiency for ethanol production remains a major challenge because of the difficulty of C–C coupling and the competitive formation of C1 products. Copper-based catalysts have demonstrated the potential for facilitating C–C coupling, but their selectivity for ethanol is often low, requiring significant overpotentials.[1,2]

To address these challenges, the teams led by Bing Joe Hwang (National Taiwan University of Science and Technology, NTUST), Wei-Nien Su (NTUST), and Meng-Che Tsai (National University of Tainan) demonstrated a dual single-atom catalyst (SAC) system featuring atomically dispersed Ni and Cu sites (NiCu-SACs/N-C), which synergistically enhance ethanol selectivity and catalytic efficiency. **Figure 1(a)** illustrates the rational design and synthesis of NiCu-SACs/N-C prepared *via* hydrothermally assisted pyrolysis using zeolitic imidazolate frameworks. The synthetic strategy ensures the atomic dispersion of Ni and Cu in a nitrogen-doped carbon matrix, creating abundant accessible active sites. To further elucidate the role of cooperative dual active sites, control experiments in CO-saturated electrolytes were conducted. The results confirm that Ni sites generate labile CO intermediates, which diffuse to adjacent Cu sites for C–C coupling, thereby forming ethanol. A key highlight of this work is the use of Ni–Cu cooperative heteroactive sites, which uniquely facilitate CO_2 reduction to ethanol with an unprecedented Faradaic efficiency (FE) of 92.2% at −0.6 V vs. reversible hydrogen electrode (RHE) (**Fig. 1(b)**). To the authors' knowledge, this represents the highest selectivity reported to date for direct electrochemical CO_2-to-ethanol conversion. The dual-atom catalyst also exhibits the lowest onset potential for ethanol production at −0.4 V vs. RHE, surpassing the performance of single-atom Cu or Ni catalysts. This exceptional performance is attributed to the cooperative entanglement of adjacent Ni and Cu sites, where CO generated on $Ni–N_3$ sites is efficiently transferred to $Cu–N_4$ sites for C–C coupling, ultimately leading to ethanol formation.

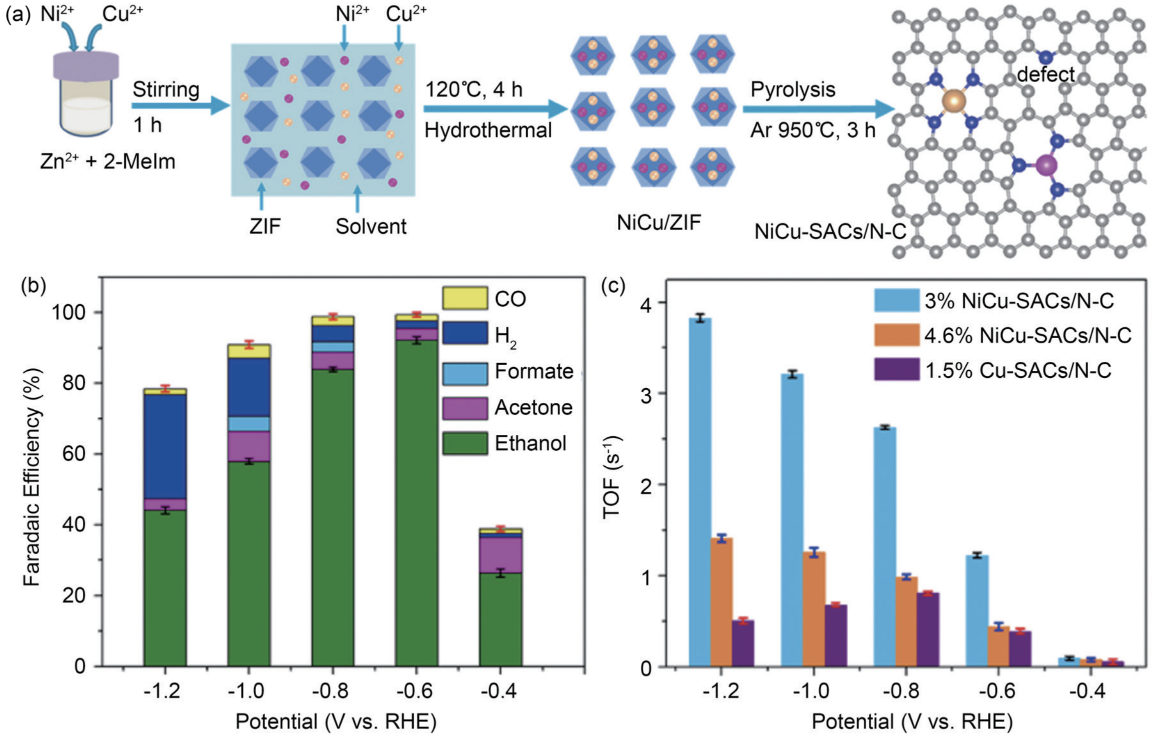

Fig. 1: (a) Schematic representation of the synthesis of dual SACs *via* hydrothermally assisted pyrolysis method. (b) FEs and product distributions over the catalysts of 3% NiCu-SACs/N-C electrodes at different potentials. Error bars indicate the standard deviation. (c) TOF of ethanol over NiCu-SACs/N-C hybrids with different metal loadings, compared with Cu-SACs/N-C at different applied potentials. [Reproduced from Ref. 3]

Figure 1(c) highlights the turnover frequency (TOF) of CO_2-to-ethanol conversion, with the NiCu-SACs/N-C catalyst exhibiting a TOF four times higher than single-atom Cu catalysts. The cooperative synergy between Ni and Cu is also evident in the significantly enhanced electrochemical active surface area and reduced charge transfer resistance (R_{ct}), indicating more efficient electron and mass transport. The computational modeling further supports the experimental findings by demonstrating that the energetically favorable C–C coupling step occurs at the $Cu–N_4$ sites, which are enhanced by neighboring $Ni–N_3$ sites. At greater negative potentials, the formation of Cu clusters increases the energy barrier for C–C coupling, leading to a decline in ethanol selectivity. This mechanistic insight explains the volcano-shaped ethanol FE trend observed in the electrochemical studies.

The role of *in situ* X-ray absorption spectroscopy (XAS) is crucial in unraveling the mechanistic insights of this dual-site catalyst. **Figure 2** presents *in situ* extended X-ray absorption fine structure (EXAFS) and X-ray absorption near-edge structure (XANES) analyses. The results reveal a key structural transformation during CO_2 reduction. Notably, while Ni remains in its single-atom $Ni–N_3$ coordination environment throughout the reaction, Cu undergoes dynamic restructuring, forming potential-induced Cu clusters at high negative potentials. These dynamic Cu clusters play a critical role in modulating catalytic activity, but excessive clustering leads to decreased ethanol selectivity. This observation, which is supported by density functional theory (DFT) calculations, confirms that C–C coupling occurs preferentially on atomically dispersed $Cu–N_4$ sites rather than Cu clusters, explaining the decline in ethanol FE at highly negative potentials.

In summary, this study establishes NiCu-SACs/N-C as a groundbreaking dual-site catalyst for CO_2-to-ethanol conversion, achieving record-high FE and low onset potential. The findings underscore the importance of cooperative single-atom site engineering and the synergistic role of Ni and Cu in promoting selective C–C coupling. The insights gained from *operando* XAS at **TPS 44A**, electrochemical analysis, and DFT modeling pave the way for designing next-generation electrocatalysts for carbon-neutral fuel production. This work provides a scalable and sustainable strategy for high-selectivity electrochemical CO_2 conversion, contributing to advancements in renewable energy and carbon capture technologies. (Reported by Hao Ming Chen, National Taiwan University)

This report features the work of Bing Joe Hwang, Wei-Nien Su and Meng-Che Tsai published in Appl. Catal. B-Environ. ***358****, 124420 (2024).*

TPS 44A Quick-scanning X-ray Absorption Spectroscopy

- *In situ* XAS
- Materials Science, Electrocatalyst

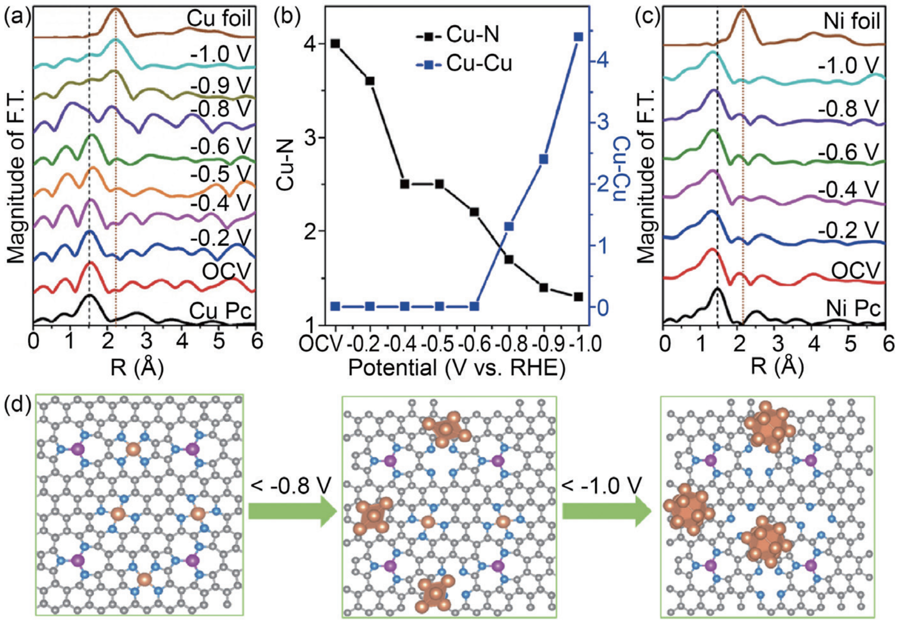

Fig. 2: (a) *In situ* EXAFS spectra and (b) the corresponding average coordination number for Cu–N and Cu–Cu shells of the Cu K-edge for 3% NiCu-SACs/N-C hybrid recorded during the CO_2 electrolysis at different applied potentials in CO_2-saturated 0.5 M $KHCO_3$. Data for CuPc and Cu foil are included for reference. (c) *In operando* EXAFS spectra of Ni K-edge for 3% NiCu-SACs/N-C hybrid recorded during the CO_2 electrolysis at different applied voltages. Data for NiPc and Ni foil are included for reference. (d) The structural models of atomically distributed Ni and Cu sites, as well as the potential-induced dynamic Cu clusters from Cu single atoms, as suggested by *in operando* analysis during the CO_2 electrolysis. [Reproduced from Ref. 3]

References

1. P. Grosse, D. Gao, F. Scholten, I. Sinev, H. Mistry, B. RoldanCuenya, Angew. Chem. Int. Ed. **57**, 6192 (2018).
2. P.-P. Yang, X.-L. Zhang, F.-Y. Gao, Y.-R. Zheng, Z.-Z. Niu, X. Yu, R. Liu, Z.-Z. Wu, S. Qin, L.-P. Chi, Y. Duan, T. Ma, X.-S. Zheng, J.-F. Zhu, H.-J. Wang, M.-R. Gao, S.-H. Yu, J. Am. Chem. Soc. **142**, 6400 (2020).
3. S. A. Chala, K. Lakshmanan, W.-H. Huang, A. W. Kahsay, C.-Y. Chang, F. T. Angerasa, Y.-F. Liao, J.-F. Lee, H. Dai, M.-C. Tsai, W.-N. Su, B. J. Hwang, Appl. Catal. B-Environ. **358**, 124420 (2024).